Non-random, individual-specific methylation profiles are present at the sixth CTCF binding site in the human H19/IGF2 imprinting control region

J. Tost, Hélène Jammes, J.M. Dupont, C. Buffat, B. Robert, T.M. Mignot, F. Mondon, Benjamin Carbonne, U. Simeoni, Guylain Grange, et al.

Non-random, individual-specific methylation profiles are present at the sixth CTCF binding site in the human *H19/IGF2* imprinting control region

Jörg Tost*, Hélène Jammes[1,2], Jean-Michel Dupont[1,3], Christophe Buffat[4], Brigitte Robert[1], Thérèse-Marie Mignot[1], Françoise Mondon[1], Bruno Carbonne[1,5], Umberto Siméoni[4], Gilles Grangé[6], Antoine Kerjean[1], Françoise Ferré[1], Ivo Glynne Gut and Daniel Vaiman[1,7]

Laboratoire d'Epigénétique, Centre National de Génotypage, 2 rue Gaston Crémieux, 91000 Evry, France, [1]Génomique et Epigénétique des Pathologies Placentaires (GEPP) INSERM U567 and UMR CNRS 8104, Hôpital Cochin and Université Paris V-René Descartes, 24 rue du Faubourg St Jacques, 75014 Paris, France, [2]Département PHASE, Institut National de la Recherche Agronomique, INRA, France, [3]Laboratoire d'Histologie, Embryologie, Cytogénétique, Faculté de Médecine, APHP, Hôpital Cochin, 123 Boulevard de Port-Royal, 75014 Paris, France, [4]Faculté de Médecine, Université de la Méditerrannée et Service de Néonatologie, Hôpital de la Conception, AP-HM, 147 Boulevard de la Baille, 13385 Marseille, France, [5]Service de Gynécologie Obstétrique, Hôpital St Antoine, 184, rue du Faubourg St-Antoine, 75012 Paris, France, [6]Service de Gynécologie Obstétrique, APHP, Hôpital Cochin, 123 Boulevard de Port-Royal, 75014 Paris, France and [7]Animal Genetics Department, Institut National de la Recherche Agronomique, INRA, France

ABSTRACT

Expression of imprinted genes is classically associated with differential methylation of specific CpG-rich DNA regions (DMRs). The *H19/IGF2* locus is considered a paradigm for epigenetic regulation. In mice, as in humans, the essential *H19* DMR—target of the CTCF insulator—is located between the two genes. Here, we performed a pyrosequencing-based quantitative analysis of its CpG methylation in normal human tissues. The quantitative analysis of the methylation level in the *H19* DMR revealed three unexpected discrete, individual-specific methylation states. This epigenetic polymorphism was confined to the sixth CTCF binding site while a unique median-methylated profile was found at the third CTCF binding site as well as in the *H19* promoter. Monoallelic expression of *H19* and *IGF2* was maintained independently of the methylation status at the sixth CTCF binding site and the *IGF2* DMR2 displayed a median-methylated profile in all individuals and tissues analyzed. Interestingly, the methylation profile was genetically transmitted. Transgenerational inheritance of the *H19* methylation profile was compatible with a simple model involving one gene with three alleles. The existence of three individual-specific epigenotypes in the *H19* DMR in a non-pathological situation means it is important to reconsider the diagnostic value and functional importance of the sixth CTCF binding site.

INTRODUCTION

Imprinted genes are expressed from only one of the parental chromosomes (1,2). Generally they are located in clusters and epigenetically marked by DNA methylation, histone acetylation/deacetylation and histone methylation and often associated with antisense RNAs (3,4). In mice, extensive studies of the paradigmatic imprinted *H19/Igf2* region revealed that the physical contacts between differentially methylated regions (DMRs), containing insulators, silencers and activators, lead to transcriptional regulation of both *H19* and *Igf2* genes (5,6). Methylation of the paternally derived allele at an imprinting control region (ICR) located 2 kb upstream of *H19* (*H19* DMR) is required to silence *H19* and to activate *Igf2* on the chromosome of paternal origin. Reciprocally, absence of methylation on the maternal allele in the *H19* DMR leads to expression of the maternal *H19* allele and the silencing of *Igf2* throughout development (7). Mechanistically, the *H19* DMR is the biological target for

CTCF, a zinc finger CCCTC-binding factor, which can bind to four sites on the unmethylated maternal *H19* DMR (8,9). The binding of CTCF creates a physical boundary on the maternal allele and inhibits interaction of downstream enhancers with *Igf2* promoters (10). In addition, CTCF binding to *H19* DMR might be necessary to prevent *de novo* methylation of the maternal allele (11).

Comparative analysis of a paternal-specific methylation imprint at the human *H19* locus revealed the presence of several highly similar 400 bp repeats containing CpG islands, although no significant sequence homology to the corresponding region of the mouse *H19* DMR could be identified (12). Much less is known about the functional regulation in humans compared to mice. The human *H19* DMR encompasses seven different binding sites for CTCF. Only the sixth CTCF binding site has been reported to act as a key regulatory domain for switching between *H19* and *IGF2* expression, whereas the other sites appear to be hyper-methylated in a study by Takai *et al.* (13). Anomalies in methylation patterns of the *H19/IGF2* locus have been consistently proposed as epigenetic markers of human disease (14–18).

However, the correlation between *H19* DMR methylation and expression is not always strictly defined. In normal human brain, biallelic expression of *IGF2* and/or *H19* is found despite differential methylation and CTCF binding (19). Also an inter-individual variability in *IGF2* imprinting with biallelic expression has been observed in lymphocytes of ∼10% of normal individuals (20). In addition, a familial aggregation of 'abnormal methylation' in ∼7% of analyzed samples was identified at the sixth CTCF binding site (21). These studies suggest overall that the regulation of methylation near imprinted genes might be leakier in human compared to mice.

Imprinted genes are probably the most important buffering factors for regulating the day-to-day trades between mother and foetus in placental mammals. Therefore understanding their regulation is of particular importance for understanding human placental physiopathology. Expression and gene invalidation data demonstrate the great importance of the *H19/IGF2* locus in placental development and physiology (22–24). Both genes are expressed at very high levels and with high specificity in human placenta (25). In this tissue, the analysis of the *H19* DMR methylation profile yielded contrasting results, with either an early monoallelic expression of *H19* established as soon as the first trimester (8–12 weeks) (26) or a progressive acquisition of monoallelic expression between the first trimester and normal term (∼39 weeks) (27). This discrepancy between the methylation of *H19* DMR and expression of *H19/IGF2*, raises the general question of the correlation and anteriority between DNA methylation, histone modification, and the ultimate mark of imprinting, monoallelic expression.

Due to the high expression of both genes in placenta and its importance in placental development, we chose to analyze systematically methylation patterns at the sixth CTCF binding site in DNAs extracted from placentas of two developmental stages in a normal population. We further analyzed lymphocyte DNA as a second tissue to identify tissue-specific effects. DNA methylation patterns are mainly investigated by cloning and subsequent sequencing, a time consuming process restricting the number of analyzed molecules to the order of tens. Recently, the pyrosequencing technology was developed and validated for DNA methylation analysis of numerous individual samples providing excellent quantitative resolution (28–30).

In this study we demonstrate the existence of three individual-specific methylation profiles in human lymphocyte DNA as well as in placenta at the sixth CTCF binding site. This observation, although not correlated with a loss of monoallelic expression of *H19* and *IGF2* raises important questions about the functional importance of the sixth CTCF binding site in humans as well as its implication in regulation at this locus. Furthermore, we can show that the three levels of methylation could be explained by a genetic model involving a unique effecting locus. This represents the first example of transgenerational heritability of DNA methylation levels in a human non-pathological situation. Finally, these results further challenge the diagnostic value of methylation profiles in the *H19/IGF2* imprinting control region as a marker for cancer or epigenetic diseases such as the Beckwith–Wiedemann or Silver–Russell syndrome.

MATERIALS AND METHODS

Sample collection

Sample collection (blood, placental villi and spermatozoa samples) was performed under a protocol approved by the institutional ethics committee. No individual identifiers or history, other than lack of known malformations were recorded. Informed consent was obtained from all individuals for the use of samples of placenta, blood and spermatozoa. Fifteen early term (between 8 and 14 weeks of amenorrhoea) and 40 full term placentas (37–40 weeks of amenorrhea) were analyzed. In 29 cases, the placenta-maternal blood sample pair was collected. In 10 cases, the placenta-cord blood and maternal blood samples were collected. Blood DNA samples from 37 individuals from 6 two- to four- generation families and from a second independent cohort of 19 adult patients were collected and analyzed. DNAs of 30 individuals from 8 families extracted from lymphoblastoid cell lines of the CEPH/Utah collection were obtained from the DNA banking facility of the CNG (Evry, France). In addition, spermatozoa from 10 normozoospermic individuals were collected.

Nucleic acid isolation

Genomic DNA was isolated from adult lymphocytes, from dissected and washed placental villi and from spermatozoa by incubation with proteinase K (0.2 mg/ml) in Lysis Saline Buffer following standard methods. RNA extraction was performed from placental villi using Trizol reagent (Invitrogen Life Technology, Cergy, France).

Methylation assays

The bisulphite conversions of genomic DNA (1 µg) and pyrosequencing analysis were performed as previously described (29,30). Supplementary Table 1 lists the accession numbers and nucleotide positions of the analyzed regions, the PCR primers and annealing temperatures used, the size of the PCR products and the number of CpGs analyzed. Primers for PCR amplification, pyrosequencing and primer extension

reactions were purchased from Biotez (Buch, Germany). Briefly, 50 ng of bisulphite converted DNA was added as template into PCR buffer with 1 mM $MgCl_2$, 200 µM dNTP, 0.4 µM of each forward and reverse biotinylated primer and 2.0 U Platinum *Taq* polymerase (Invitrogen Life Technology). The PCR program consisted of a denaturing step of 4 min at 95°C followed by 50 cycles of 30 s at 95°C, 30 s at the hybridization temperature (see Supplementary Table 1) and 20 s at 72°C, with a final extension of 5 min at 72°C. Purification of the PCR product with streptavidin Sepharose® HP beads (GE Healthcare, Uppsala, Sweden) and hybridization of the biotinylated PCR products and the sequencing primer were conducted following the PSQ96 sample preparation guide using a vacuum filtration sample transfer device (Pyrosequencing AB, Uppsala, Sweden). Sequencing was performed on a PSQ 96MA system with the PyroGold SQA reagent kit according to the manufacturer's instructions (Pyrosequencing AB). All PCRs were checked for the absence of preferential amplification by mixing known ratios of whole-genome amplified and *in vitro* methylated (SssI, Ozyme, St Quentin-en-Yvelines, France) DNA. Pyrosequencing primers and templates were controlled for self-extension or primer-dimer formation.

The verification of the methylation status of selected CpG positions was performed by MALDI mass spectrometry as previously described (29,31). For cloning and sequencing, the PCR products were subcloned into a TA cloning vector (pGemT vector, Promega, Charbonnieres, France) according to manufacturer's instructions and 30 clones were selected for sequencing.

Allele-specific expression

Allele-specific expression was carried out by genotyping of the RsaI polymorphism (rs3741219) in exon 5 of *H19* and the ApaI polymorphism (rs680) in exon 9 of *IGF2*, respectively. RT–PCR products were analyzed for samples heterozygous for the respective SNPs (n = 34 for *H19* and n = 10 for *IGF2*, respectively). Primers are listed in Supplementary Table 2. After the cDNA synthesis, PCR products were either analyzed by standard Sanger sequencing on a 3730 ABI sequencer using the above described primer set (rs3741219, rs2839704 and rs2839703) for the *H19* gene, or digested by ApaI and electrophoresed on a 2% agarose gel to analyze the *IGF2* polymorphism.

Quantitative RT–PCR

Real-time PCR was performed using a Lightcycler (Roche[TM] Diagnostics, Mannheim, Germany) and SYBR Green master mix (Invitrogen) to quantify gene expression. Primers (Supplementary Table 2) were designed to amplify a region encompassing exons 7, 8 and 9 of *IGF2* and a region in exon 5 of *H19*. Relative expression of *IGF2* and *H19* is shown normalized to the expression of the succinate dehydrogenase A (SDHA).

Genotyping of polymorphisms

Genomic DNA was analyzed for two SNPs (rs10732516 and rs 2071094) and RT-PCR products were analyzed for three SNP (rs2839703, rs2839704 and rs3741219). Genotyping of polymorphisms were performed by pyrosequencing using the SNP genotyping kit according to the manufacturer's instructions (Pyrosequencing AB).

Statistical analysis

A Mann–Whitney rank test was used to determine whether the epigenotypes (hypo-, median- and hyper-methylated profiles) were associated with tissue type (placenta versus lymphocytes) and to test the distribution of the *H19* and *IGF2* expressions in early term and full-term placentas. A Monte Carlo based permutation test was used to evaluate the statistical significance of the distribution of the methylation profiles to exclude random effects. Student's *t*-test was used to test the significance of gene expression differences between groups. A χ^2 test was used to determine whether the proportion of the different genotypes (CC, TT and CT, SNP rs10732516) was similar in the general population and in individuals analyzed in this study.

RESULTS

Methylation analysis of the sixth CTCF binding site in the *H19* DMR

We analyzed the methylation levels at sixteen consecutive CpGs at the sixth CTCF binding site in the *H19* DMR in DNA from lymphocytes (maternal blood cells, blood 1) as an adult control tissue, and in DNA from human placentas at two different stages of placental development (early gestation, 8–14 weeks of amenorrhea, or at full term gestation, 37–40 weeks of amenorrhea) by pyrosequencing. While an overall methylation level of 50% was expected, a high variability of methylation levels between individuals and consecutive CpGs was found leading to a surprisingly complex methylation pattern in both adult lymphocytes and placentas (Figure 1A–C). The fifth CpG in the DMR was completely unmethylated for some samples, which is explained by the existence of a C/T SNP (rs10732516). DNA samples harboring a T were therefore completely unmethylated, which explains the dip in the methylation level at this position for several of the DNA samples. This polymorphism did not affect the global methylation level of the DMR. After exclusion of the fifth CpG the methylation profiles in the *H19* DMR could be grouped into three discrete methylation categories in maternal blood cell DNA (Figure 1A): a hyper-methylated profile (average methylation > 66%: 80.2 ± 8.2%), a median-methylated profile (33% < average methylation < 66%: 44.5 ± 5.1%) and a hypo-methylated profile (average methylation < 33%: 17.7 ± 7.5%). The median-methylated profile was encountered in 59% of the lymphocyte samples, while the hypo- and hyper-methylated represented 28% and 13%, respectively. A Monte-Carlo based permutation test (n = 5000) was used to test objectively for this discrete distribution into three categories (from 0 to 33%, from 33 to 66% and from 66 to 100% of methylation, respectively). Compared with the simulated dataset, probabilities of $P < 0.008$, $P < 0.002$ and $P < 0.03$ were obtained for the three categories, respectively. It can thus be concluded that the repartition was non-random and results from genuine biological differences. To exclude any sampling bias, we confirmed the distribution of the methylation status in a second independent cohort of nineteen adult individuals (Figure 1D, blood 2).
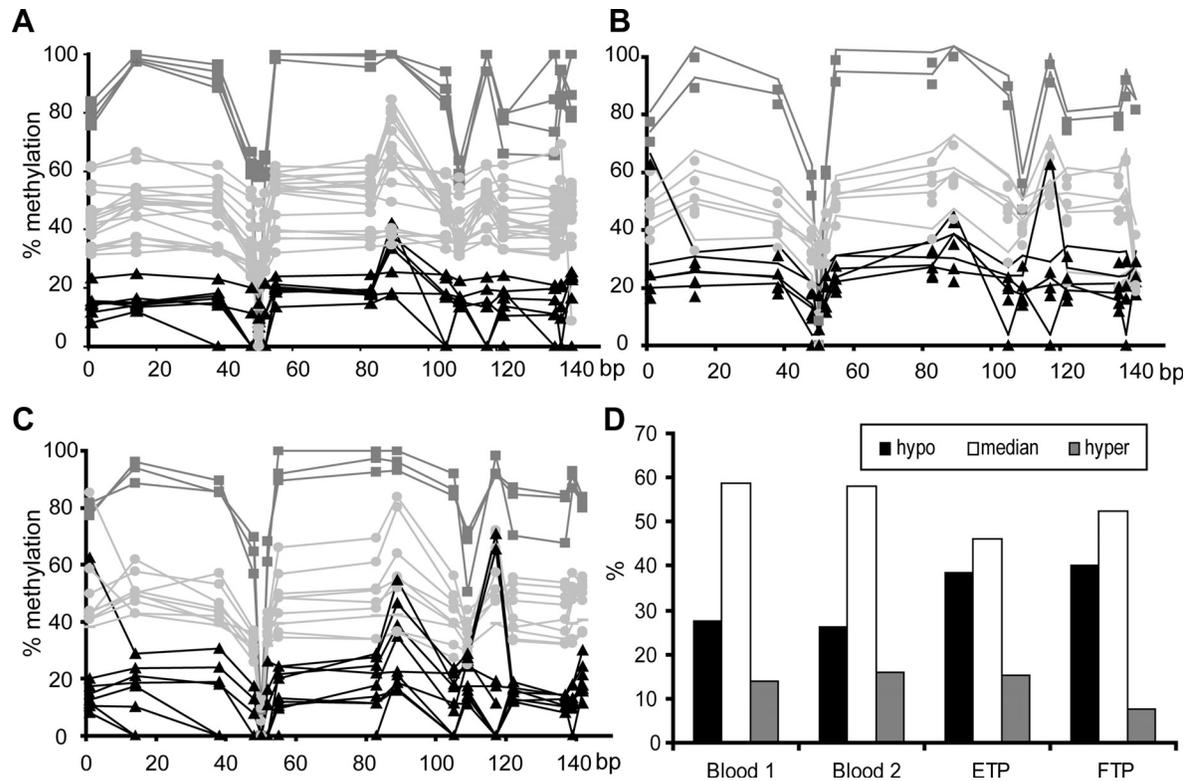
Figure 1. Profiles of *H19* DMR methylation obtained by pyrosequencing in maternal lymphocyte DNA samples (**A**, Blood 1, $n = 29$) and in placenta DNA samples at early term (**B**, ETP, $n = 15$) and full term of gestation (**C**, FTP, $n = 40$ analyzed; $n = 20$ represented). A similar distribution was found in placenta and the two cohorts of lymphocytes (Blood 1 and Blood 2, **D**). The fifth CpG analyzed corresponds to a C/T polymorphic position in the CTCF binding site (rs10732516).

Further investigation revealed that these levels were not restricted to lymphocyte DNA. Similar profiles were also observed in placental tissue DNA (Figure 1B and C), albeit with a less clear division between the hypo- and median-methylated profiles, consistent with the classical observation of a placental hypo-methylation compared to other tissues. The frequencies of the three epigenotypes were not different between the two independent cohorts of lymphocyte DNAs (maternal or from anonymous adult individuals), early term or full term placentas (Figure 1D). Also inside each methylation group the inter-individual variations were not significantly different between placenta and lymphocyte samples.

The parental origin of the methylated strands was addressed by cloning and Sanger sequencing of PCR products from three placental samples corresponding to each one of the three different methylation profiles and heterozygous for the single nucleotide polymorphism rs2071094 (Figure 2). The hyper-methylated profile corresponds mainly to methylated DNA molecules from both the maternal and paternal origin. Similarly, the hypo-methylated profile corresponded mainly to unmethylated molecules from both parental alleles. Consistent with the classical model, the median-methylated profile corresponded to the presence of methylated molecules of paternal origin.

Validation of the epigenetic profiles at the sixth CTCF binding site

Since our results were unexpected and somewhat contradictory to published observations of the homologous mouse DMR, we controlled and reproduced the results to exclude any technical artefacts in addition to the cloning and sequencing experiment described above.

(i) To rule out incomplete bisulphite conversion of the genomic DNA, the bisulphite treatments were standardized and verified. Systematically, 1 µg of genomic DNA was used for bisulphite conversion and 50 ng of converted DNA for PCR amplification. Conversion rates were confirmed by cloning and sequencing PCR products. This revealed that >99% of unmethylated cytosines were converted. Four independent replicates of the bisulphite treatment followed by PCR amplification were carried out for six placental DNA samples, displaying a very good reproducibility of the process (SD < 5.0%; Supplementary Figure 1A). The same methylation profiles were obtained using a second primer set encompassing the previous primer positions ($n = 6$, Supplementary Figure 1B).

(ii) Since the structure of the *H19* DMR is very complex and consists of highly similar repeats (12), the specificity of the amplified PCR products was checked by systematically reanalyzing the amplified sequence at each base pair to demonstrate that the DMR encompassing the sixth CTCF binding site was exclusively amplified. Supplementary Figure 2 shows the alignment of the different consecutive binding sites proving that the sixth CTCF site is clearly distinguishable from the others after pyrosequencing. Any additional or missing base in the analyzed sequence—even partially—would induce
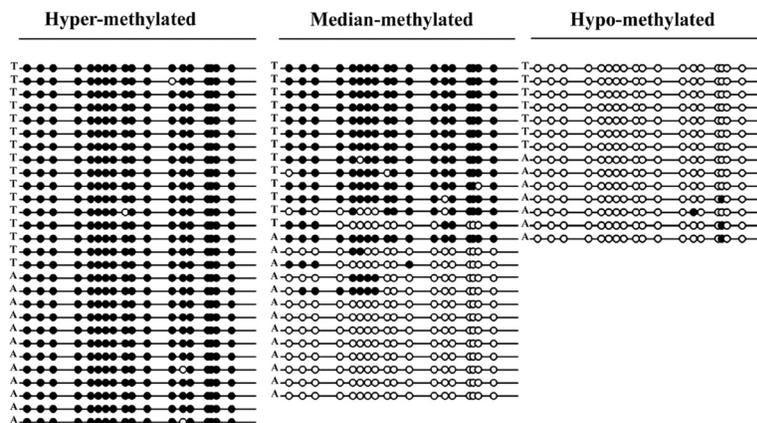
Figure 2. Cloning and Sanger sequencing of PCR products from three placental samples corresponding to the three different profiles. SNP rs2071094 was used to determine the parent-of-origin of the methylated alleles.
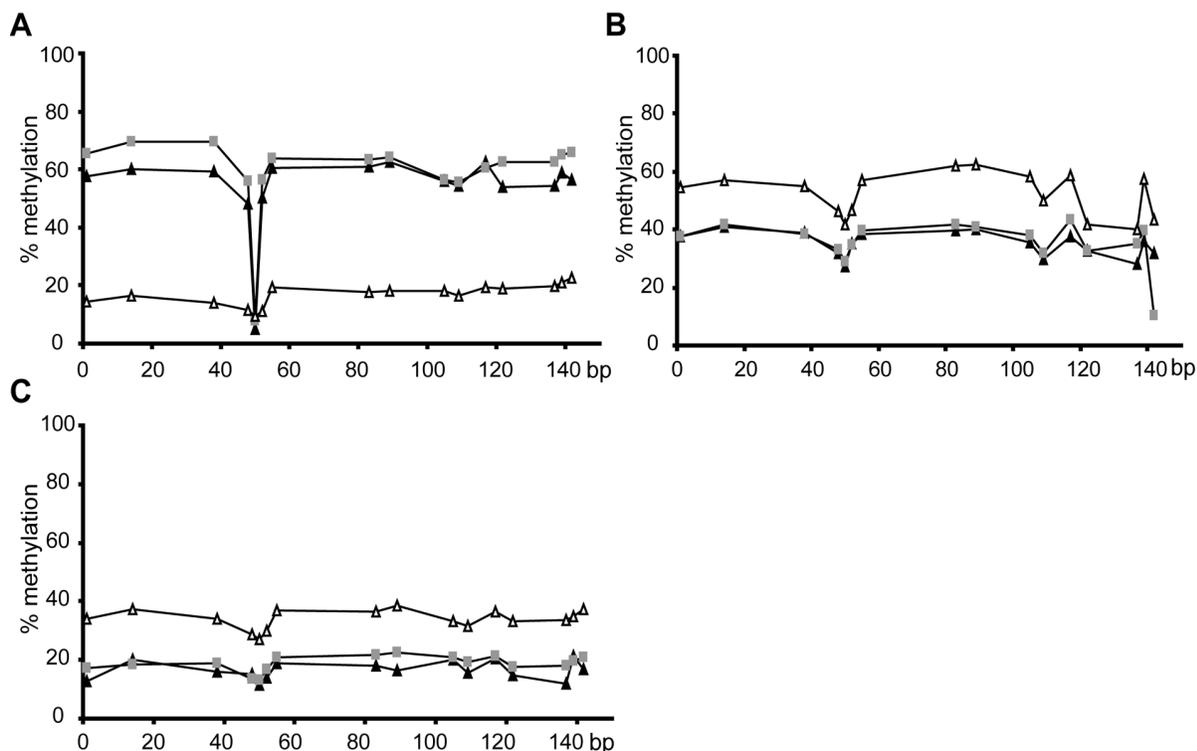

Figure 3. Methylation profiles at the sixth CTCF binding site in placental (closed squares) and foetal lymphocyte DNA (closed triangles) samples in comparison to the maternal lymphocyte DNA samples (open triangle) for three different mother-child pairs.

failure of the pyrosequencing procedure, which is based on the sequential input of the correct nucleotides into the elongating DNA strand.

(iii) Results were further confirmed by an independent quantitative method using a single base primer extension assay combined with MALDI mass spectrometric detection for several CpG inside the analyzed DMR (31).

The methylation level of the *H19* DMR is individual-specific but does not depend on the tissue analyzed

We analyzed DNAs originating from the placenta and from blood of the foetus, taken at the time of birth for 10 individuals. The methylation profile was found to be identical in the two different tissues from the same individual (Figure 3). This showed that the epigenotype (hypo-, median- or hyper-methylated) is acquired early in development, probably before the separation of the syncytiotrophoblast from the inner cell mass. This early determination supports a strict determinism of the methylation status, which is maintained through the individual's life.

Familial transmission of *H19* DMR epigenotypes

The literature evoked the existence of 'aberrant' familial aggregation of methylation at the sixth CTCF binding site (21). Since different epigenotypes were often observed
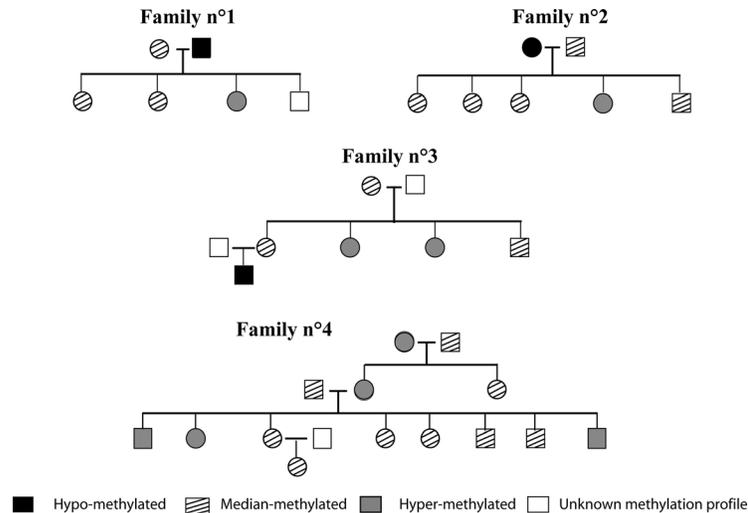
Figure 4. Familial segregation of individuals with various methylation profiles analyzing DNA samples from fresh blood.

in the analysis of the mother/placenta pairs, we envisaged that these different epigenotypes could be due to familial segregation of 'methylated' alleles. Therefore we tested the possibility of genetic transmission of the three observed methylation levels. We analyzed the epigenetic profiles of 6 two- to four-generation families encompassing a total of 37 children (Figure 4, only the four most informative families are presented), as well as the epigenotypes of 29 mother/placenta pairs. When considering the transmission pattern from parents (both sexes) to children, 83 transmissions could be followed, which were 9 hypo-, 52 median- and 22 hyper-methylated. In a random situation, the epigenotype of the descendant would not be influenced by the epigenotype of the parent. Under this hypothesis, for a given child epigenotype, the probability of each parent epigenotype is 1/3. In fact, the actual proportions varied according to each epigenotype. These proportions were tested by a χ^2 test and were found to be highly significant ($P = 0.00014$). This indicated that the transmission from parent to child was not random. In addition, we tested the epigenotypes of lymphocytes from 48 unrelated individuals (blood 1 and blood 2 cohorts), yielding 27, 59 and 14% of hypo-, median- and hyper-methylated epigenotypes, respectively. This sample was used as a reference population. These proportions were markedly different from that observed in our six families ($P = 0.0006$). These data showing different proportions in familial structures compared to a cohort of unrelated individuals strengthen the hypothesis of a genetic transmission of the epigenotypes. Without exception, our familial transmission patterns were compatible with a model of a single gene presenting three alleles and a strict model of dominance: median- > hypo- > hyper-methylated. The model was compatible with Hardy–Weinberg equilibrium.

In order to further validate the likelihood of our model we tried to follow methylation profiles in families from the CEPH-Utah collection analysing 30 different individuals from 8 families. However, all samples displayed a median-methylated profile with an average methylation of 38%. This homogeneity has probably been acquired during immortalization of the cells or cell culture.

To test for a correlation between the genetic structure of the locus and the methylation profile we compared genotype data from haplotype-tagging SNPs in the DMR upstream of *H19*, in *H19* itself and in *IGF2* (J. Tost, unpublished data) to the epigenetic profile, but no association was found. In DNA from purified spermatozoa, the analysis of the *H19* DMR methylation profile by pyrosequencing showed complete hyper-methylation, as expected for spermatozoa ($n = 10$). This suggests that the individual-specific methylation status of *H19* DMR observed in lymphocytes and in placentas is acquired after fertilization during the differentiation of somatic cell lineages.

Spatial extension of the three methylation profiles

Methylation profiles are restricted to the sixth CTCF site. To determine the extent of the variable epigenetic profiles, we analyzed 10 CpGs encompassing the third CTCF site (Figure 5) as well as 9 CpGs in the direct proximal promoter region of *H19*. All samples displayed ∼40% methylation at these two loci.

Methylation status of IGF2 DMR2 is independent of the epigenotype at the sixth CTCF site in the H19 DMR. In mice, the *H19* DMR is needed on the maternal allele to protect the *Igf2* DMR1 and 2 from methylation (7). To assess a putative link of the methylation level at the sixth CTCF site of the *H19* DMR with the methylation level in the *IGF2* DMR2 we analyzed the methylation status of the *IGF2* DMR2 by pyrosequencing. Two regions encompassing 17 CpGs (278 bp, *IGF2* DMR2a) and 9 CpGs (195 bp, *IGF2* DMR2b), separated by 265 bp and located in exons 8 and 9 of *IGF2* (Figure 6) were quantitatively screened for individual-specific differential methylation. A highly specific and reproducible profile was observed for the DMR, irrespective of the sample used (placentas or maternal blood cells). Strong variability of methylation was observed between consecutive CpGs. The average proportion of methylated molecules in the first region (*IGF2* DMR2a) was 62.9 ± 7.3% in lymphocytes (maternal blood cells, MBC), 47.5 ± 4.9% in early gestation placenta (ETP) and 41.1 ± 5.4% in term placenta
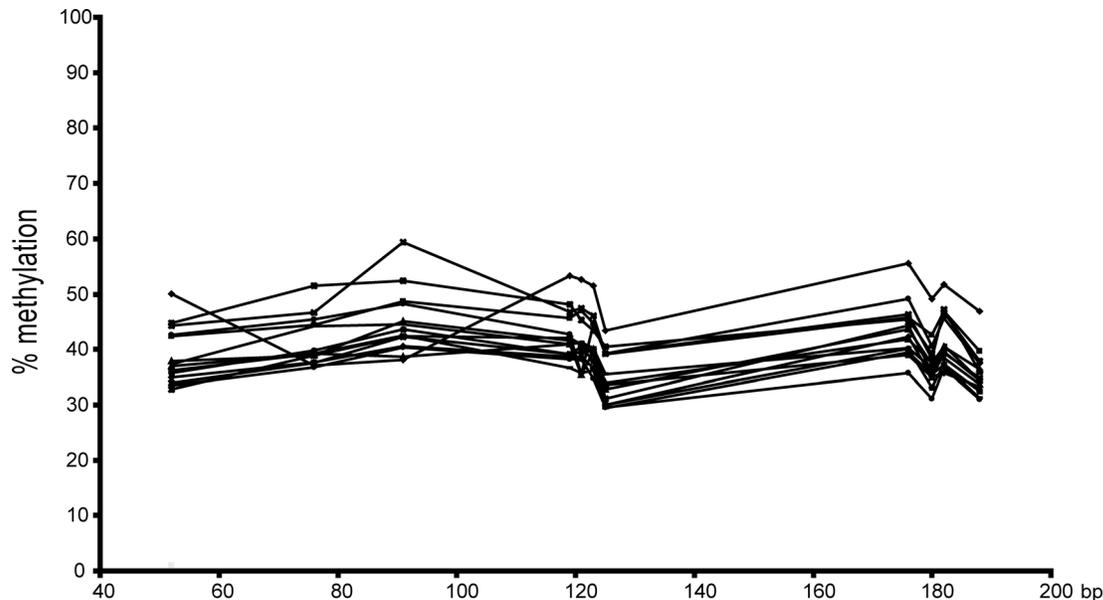
Figure 5. DNA methylation profiles of the third CTCF binding site obtained by pyrosequencing. The degree of methylation (%) was analyzed for 11 CpGs. Analysis was performed on the same samples as for the *IGF2* DMR2 (Figure 6). A unique profile was obtained. Only 14 samples are shown for clarity.

(FTP). The methylation of placenta samples was significantly lower than in adult lymphocytes ($P < 0.0001$). Similarly, the *IGF2* DMR2b was hypo-methylated in placenta samples: $35.0 \pm 8.9\%$ in ETP, $34.0 \pm 3.6\%$ in FTP and $57.4 \pm 3.9\%$ in maternal blood cells, respectively (Figure 6). Again the difference between [FTP-ETP] and MBC methylation levels was highly significant ($P < 0.0001$). By contrast, the methylation status of both DMR2a and 2b were never significantly different between early gestation and full term placentas. The comparative analysis of the *H19* and *IGF2* DMRs from the same samples revealed that their methylation levels were not correlated in humans.

Relationship between *H19* DMR epigenotypes and expression of both *H19* and *IGF2* genes in human placenta

We then addressed the question whether the epigenetic polymorphism (three profiles) at the sixth CTCF binding site had an effect on the allele-specific expression of either *H19* or *IGF2* as well as on the quantity of the mRNA of both genes. As *H19* and *IGF2* are highly expressed in placenta but not in lymphocytes, 34 placental DNA, heterozygous for the SNP rs3741219 (RsaI cleavage site) in the last exon of *H19,* were selected (Supplementary Table 3). These samples were used to follow *H19* allelic expression by RT–PCR followed by conventional Sanger sequencing. A single allele was exclusively expressed in 25 cDNA samples (83.3%) and predominantly expressed in five cDNA samples (16.7%). In this case, 80% of the cDNA molecules originated from one allele and 20% from the second. There was no correlation with the methylation profile of the corresponding genomic DNA samples (among the three samples where *H19* was not exclusively expressed from the maternal allele, one was hyper-, one was hypo-, and one was median-methylated). Similarly, samples informative ($n = 10$) for the ApaI

polymorphism in exon 9 of *IGF2* demonstrated the allele-specific expression of the gene without exception. Therefore, the imprinting status of both genes is maintained whatever the methylation profile of the sixth CTCF binding site.

We measured the overall expression levels of *IGF2* and *H19* in early gestation and full-term placental villi by quantitative RT–PCR. A very strong positive correlation was found between the *IGF2* and *H19* mRNA levels in ETP ($R^2 = 0.87$) and a less strong in FTP ($R^2 = 0.36$, Figure 7). Very clearly, both genes are expressed at a much lower level at full-term compared to early gestation placentas (Mann–Whitney test: $P = 0.008$). Finally, the overall level of *H19* and *IGF2* expression was analyzed with regard to the methylation profile of the *H19* DMR, but no significant differences could be found. In conclusion our results dissociate the methylation status of the sixth CTCF site of the *H19* DMR from the expression level of both *H19* and *IGF2* and suggest that other complementary mechanisms could be at work for maintaining a specific expression level of both genes in the placenta.

DISCUSSION

This sixth CTCF site has previously been postulated as being the only one of the seven CTCF sites that is used for imprinting control (13). Therefore, the sixth CTCF binding site might be considered as the human functional homologue of the allele-specifically methylated region in the mouse *H19/IGF2* ICR despite low sequence conservation between the two species. Our study shows that the sixth CTCF binding site is not consistently allele-specifically methylated in humans. However, the expected median-methylated pattern is found in another region of the DMR, as well as in the *H19* promoter. Our observations suggest that the sixth CTCF binding site is at least not always involved in the allele-specific expression of *H19* and *IGF2* and that either
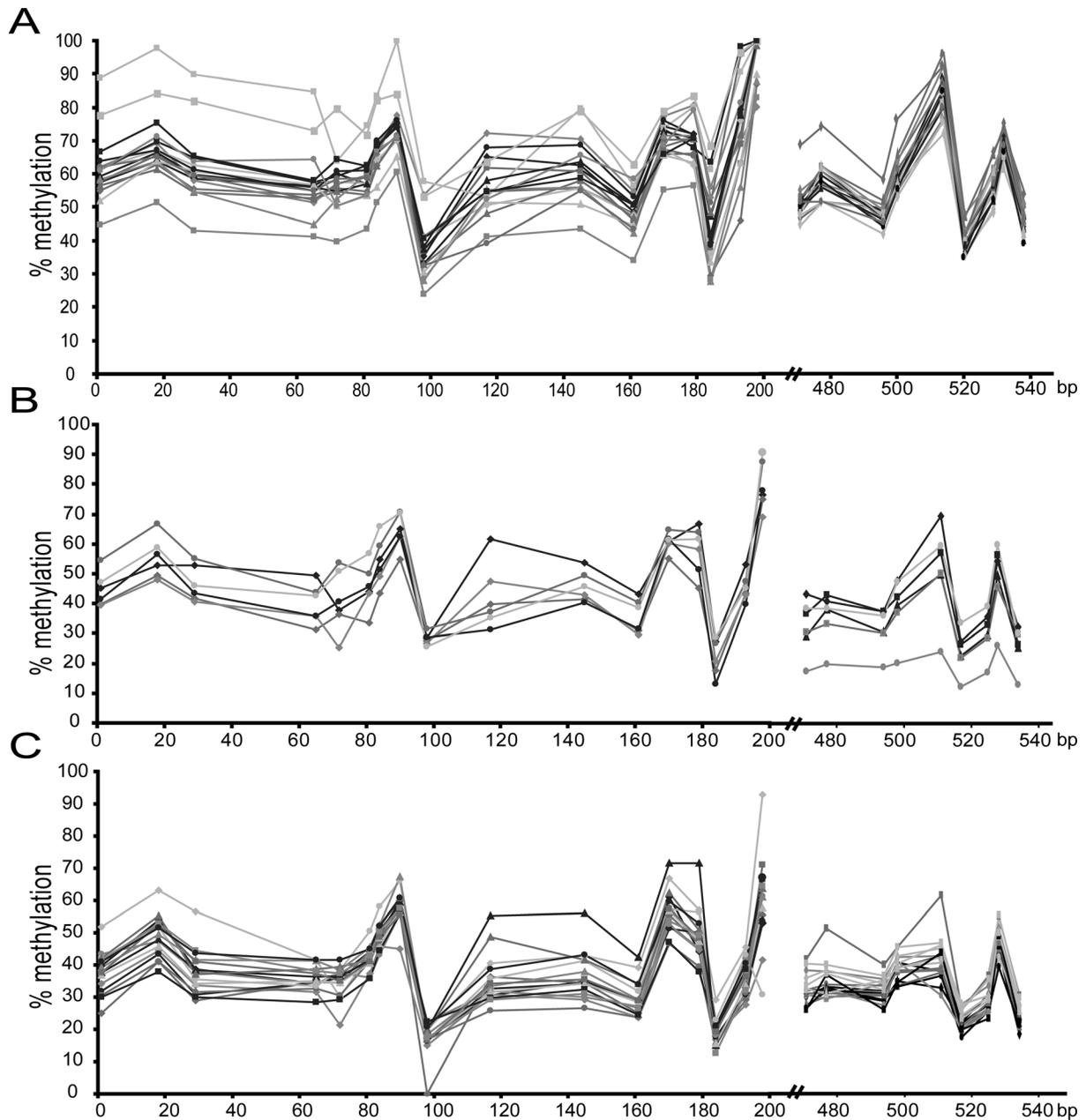
Figure 6. Profiles of *IGF2* DMR methylation obtained by pyrosequencing. The degree of methylation (%) was analyzed for two differentially methylated regions, 17 CpGs in DMR2a and 9 CpGs in DMR2b. Analysis was performed on maternal blood cell DNA samples (**A**, Blood 1 $n = 17$), on placenta samples at early term of gestation (**B**, $n = 6$) and at full term (**C**, $n = 16$).

other CTCF binding sites or an overall allele-specific methylation state of the locus determines imprinted expression. Alternatively, species-specific mechanisms might exist in the onset and/or maintenance of imprinting in different mammals. In addition, we found that the methylation profile for a given individual is determined early in development (before the division of the inner cell mass lineage and the trophectoderm lineage) and presumably genetically determined.

DNA methylation is generally addressed by cloning and DNA sequencing of PCR products from bisulphite treated DNA. This has become the standard technique for determining the methylation status of CpG imprinted regions. The major limitation of this technique is that it extrapolates methylation data from a reduced number of independently sequenced DNA molecules (generally 10–20) to a whole tissue. DNA methylation analysis by pyrosequencing has become more and more widespread as it combines important features such as ease-of-use, quantitative accuracy and high-throughput possibilities. For the presented study, the use of pyrosequencing also minimized the risk of technical artifacts. The sequences of the different CTCF sites are very similar, but do differ at some nucleotides. Any unspecific amplification of, e.g. several binding sites, would therefore be seen in the resulting pyrogram and would not pass quality control. Two recent studies demonstrated the presence of microdeletions fusing different CTCF binding sites in the *H19* DMR
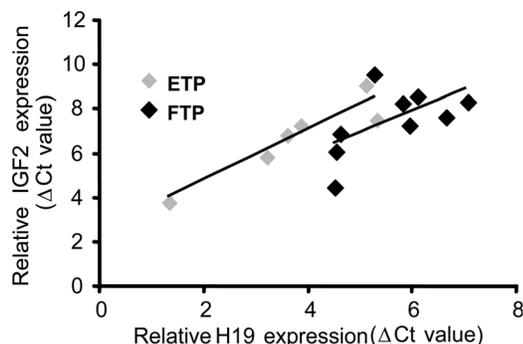
Figure 7. *H19* and *IGF2* expression levels in human placenta. Real-time quantitative PCR was performed using cDNA from 6 early- and 10 full-term placentas, respectively. Succinate dehydrogenase A (SDHA) gene expression was used as standard.

that lead to the hyper-methylation at the sixth CTCF binding site in Beckwith–Wiedemann syndrome patients (32,33). Although we can not exclude microdeletions in other parts of the DMR, we can be sure that the results are not due to a deletion or fusion of CTCF sites as this would, for the above described reasons, be visible in the obtained sequences. As the same methylation profile is found in different tissues from the same individual (blood and placenta), any artifact in the preparation of the DNA from the placentas and the lymphocytes can clearly be ruled out.

When analyzing the four functional CTCF sites in mice in ten different organs by pyrosequencing, we found a unique methylation profile in all organs as well as in the different analyzed mice (J. Tost, unpublished data). In humans, previous work showed that paternal specific methylation at *H19* DMR is very well conserved not only in tissues that have parental specific expression of the two genes, but also in tissues such as the choroid plexus where expression is biallelic (34). Our results show that the opposite situation exists, i.e. tissues where the typical imprinted pattern of expression does not directly correlate with specific methylation levels. Indeed, while a major part of the human population exhibited the expected allele-specific methylation pattern, 34 to 65%, of the human population escapes the classically described median-methylated profile of the DMR (34% in maternal lymphocytes, 43% when considering male and female adult lymphocytes, 65% in placentas).

Aberrant methylation in the *H19* DMR has previously been reported, mainly in analyses in the context of cancer. For example Cui *et al.* reported hyper-methylation at the first CTCF site in Wilms tumour with loss of imprinting, but also Wilms tumour samples with normal imprinting of *IGF2* did not necessarily show a normal pattern of methylation at the *H19* DMR. A recent study on head and neck carcinomas showed aberrant hyper-methylation at the sixth CTCF binding site in the control population (35). While Takai *et al.* (13) only found allele-specific methylation at the sixth CTCF binding site when analysing a few normal tissues, Sandovici *et al.* (21) reported on a familial aggregation of 'aberrant' methylation in a non-pathological situation. Our results support the findings reported by Sandovici *et al.* (21) which observed a sporadic or familial abnormal methylation status of *H19* DMR as well as stability of this trait over a period of nearly two decades. However, due to the method

based on methylation sensitive restriction endonucleases used in that study, they were only able to detect hyper- and median-methylated samples and therefore did not understand the full extent of the epigenetic polymorphism. By their method, a hypo-methylated profile is indistinguishable from the expected median-methylated methylation level as in both cases one allele is retrieved after digestion. Only a complete loss of methylation would result in a different result. This would also explain their higher percentage of median-methylated samples as they would have classed all but the hyper-methylated samples in this category. Their reported observations were also consistent with the possibility that a *H19* DMR epigenotype is largely due to genetic factors.

Germline transmitted epimutations has been found in several plants and two metastable transposon-associated epimutations were described in mice (36). The maternally transmitted epigenetic state of the *Agouti viable yellow* allele determines coat color (37) and a parent-of-origin independent transmission of differential methylation at an internal retrotransposon of the A*xin^Fu* allele leads to a presence or absence of the phenotype, a kinked tail (38). The only previously reported transgenerational inherited human epiallele concerns the mutL homolog 1 (MLH1) where methylated alleles confer an increased risk to develop cancer (39,40). We have shown that the observed epigenetic profiles at the sixth CTCF binding site are non-random and follow a pattern of inheritance that might be determined by a single genetic factor. Further work on familial genotyped DNAs from non-immortalized cell lines will be necessary to map the putative locus or gene responsible for the three methylation profiles and ascertain the proposed model of dominance.

Our findings suggest the absence of a direct connection between *H19* monoallelic expression and *H19* DMR allele-specific methylation at the sixth CTCF binding site. Allele-specific methylation at this locus might therefore play only a secondary role as an epigenetic mark in humans. Alternatively, it could be a primary mark early in development, which is then lost after the blastocyst stage. A contrasted situation was found in mice with respect to the imprinting centre located in the *Kcnq1* domain on distal chromosome 7. In the embryo, imprinting is stably maintained only on genes that have promoter DNA methylation whereas in the placenta, the paternal repression along this domain involves the acquisition of histone H3 methylation without the involvement of promoter DNA methylation (41,42).

The correlation between the total expression levels of *IGF2* and *H19* suggests a co-regulation by a process acting simultaneously on the two homologous chromosomes and equilibrating the amount of transcript of both genes at specific stages of developing placenta. This could for example be achieved by a limiting amount of transcription factor. This hypothesis is strengthened by a systematic bioinformatic analysis of promoters from the *H19/IGF2* locus demonstrating that the transcription factor binding site content of the P3 of *IGF2* is highly similar to that of the P1 of *H19* (D. Vaiman *et al.*, unpublished data).

In conclusion, we could demonstrate the existence of three distinct non-random individual-specific methylation levels at the sixth CTCF site in the *H19* DMR, which are probably set by a so far unidentified genetic factor. An immediate consequence of our study is the need for re-consideration of

methylation of at least the sixth CTCF site as diagnostic marker for cancer or epigenetic 'diseases' such as Silver–Russel and Beckwith–Wiedemann syndrome.

SUPPLEMENTARY DATA

Supplementary Data are available at NAR online.

REFERENCES

1. Ferguson-Smith,A.C. and Surani,M.A. (2001) Imprinting and the epigenetic asymmetry between parental genomes. *Science*, **293**, 1086–1089.
2. Reik,W. and Walter,J. (2001) Genomic imprinting: parental influence on the genome. *Nature Rev. Genet.*, **2**, 21–32.
3. Holmes,R. and Soloway,P.D. (2006) Regulation of imprinted DNA methylation. *Cytogenet. Genome Res.*, **113**, 122–129.
4. Lewis,A. and Reik,W. (2006) How imprinting centres work. *Cytogenet. Genome Res.*, **113**, 81–89.
5. Kurukuti,S., Tiwari,V.K., Tavoosidana,G., Pugacheva,E., Murrell,A., Zhao,Z., Lobanenkov,V., Reik,W. and Ohlsson,R. (2006) CTCF binding at the H19 imprinting control region mediates maternally inherited higher-order chromatin conformation to restrict enhancer access to Igf2. *Proc. Natl Acad. Sci. USA*, **103**, 10684–10689.
6. Lopes,S., Lewis,A., Hajkova,P., Dean,W., Oswald,J., Forne,T., Murrell,A., Constancia,M., Bartolomei,M., Walter,J. *et al.* (2003) Epigenetic modifications in an imprinting cluster are controlled by a hierarchy of DMRs suggesting long-range chromatin interactions. *Hum. Mol. Genet.*, **12**, 295–305.
7. Thorvaldsen,J.L., Duran,K.L. and Bartolomei,M.S. (1998) Deletion of the H19 differentially methylated domain results in loss of imprinted expression of H19 and Igf2. *Genes Dev.*, **12**, 3693–3702.
8. Bell,A.C. and Felsenfeld,G. (2000) Methylation of a CTCF-dependent boundary controls imprinted expression of the Igf2 gene. *Nature*, **405**, 482–485.
9. Hark,A.T., Schoenherr,C.J., Katz,D.J., Ingram,R.S., Levorse,J.M. and Tilghman,S.M. (2000) CTCF mediates methylation-sensitive enhancer-blocking activity at the H19/Igf2 locus. *Nature*, **405**, 486–489.
10. Lewis,A. and Murrell,A. (2004) Genomic imprinting: CTCF protects the boundaries. *Curr. Biol.*, **14**, R284–286.
11. Fedoriw,A.M., Stein,P., Svoboda,P., Schultz,R.M. and Bartolomei,M.S. (2004) Transgenic RNAi reveals essential function for CTCF in H19 gene imprinting. *Science*, **303**, 238–240.
12. Frevel,M.A., Hornberg,J.J. and Reeve,A.E. (1999) A potential imprint control element: identification of a conserved 42 bp sequence upstream of H19. *Trends Genet.*, **15**, 216–218.
13. Takai,D., Gonzales,F.A., Tsai,Y.C., Thayer,M.J. and Jones,P.A. (2001) Large scale mapping of methylcytosines in CTCF-binding sites in the human H19 promoter and aberrant hypomethylation in human bladder cancer. *Hum. Mol. Genet.*, **10**, 2619–2626.
14. Reik,W., Brown,K.W., Schneid,H., Le Bouc,Y., Bickmore,W. and Maher,E.R. (1995) Imprinting mutations in the Beckwith-Wiedemann syndrome suggested by altered imprinting pattern in the IGF2-H19 domain. *Hum. Mol. Genet.*, **4**, 2379–2385.
15. Nakagawa,H., Chadwick,R.B., Peltomaki,P., Plass,C., Nakamura,Y. and de La Chapelle,A. (2001) Loss of imprinting of the insulin-like growth factor II gene occurs by biallelic methylation in a core region of H19-associated CTCF-binding sites in colorectal cancer. *Proc. Natl Acad. Sci. USA*, **98**, 591–596.
16. Cui,H., Niemitz,E.L., Ravenel,J.D., Onyango,P., Brandenburg,S.A., Lobanenkov,V.V. and Feinberg,A.P. (2001) Loss of imprinting of insulin-like growth factor-II in Wilms' tumor commonly involves altered methylation but not mutations of CTCF or its binding site. *Cancer Res.*, **61**, 4947–4950.
17. Cui,H., Onyango,P., Brandenburg,S., Wu,Y., Hsieh,C.L. and Feinberg,A.P. (2002) Loss of imprinting in colorectal cancer linked to hypomethylation of H19 and IGF2. *Cancer Res.*, **62**, 6442–6446.
18. Gicquel,C., Rossignol,S., Cabrol,S., Houang,M., Steunou,V., Barbu,V., Danton,F., Thibaud,N., Le Merrer,M., Burglen,L. *et al.* (2005) Epimutation of the telomeric imprinting center region on chromosome 11p15 in Silver-Russell syndrome. *Nature Genet.*, **37**, 1003–1007.
19. Ulaner,G.A., Yang,Y., Hu,J.F., Li,T., Vu,T.H. and Hoffman,A.R. (2003) CTCF binding at the insulin-like growth factor (IGF2)/H19 imprinting control region is insufficient to regulate IGF2/H19 expression in human tissues. *Endocrinology*, **144**, 4420–4426.
20. Sakatani,T., Wei,M., Katoh,M., Okita,C., Wada,D., Mitsuya,K., Meguro,M., Ikeguchi,M., Ito,H., Tycko,B. *et al.* (2001) Epigenetic heterogeneity at imprinted loci in normal populations. *Biochem. Biophys. Res. Commun.*, **283**, 1124–1130.
21. Sandovici,I., Leppert,M., Hawk,P.R., Suarez,A., Linares,Y. and Sapienza,C. (2003) Familial aggregation of abnormal methylation of parental alleles at the IGF2/H19 and IGF2R differentially methylated regions. *Hum. Mol. Genet.*, **12**, 1569–1578.
22. Constancia,M., Hemberger,M., Hughes,J., Dean,W., Ferguson-Smith,A., Fundele,R., Stewart,F., Kelsey,G., Fowden,A., Sibley,C. *et al.* (2002) Placental-specific IGF-II is a major modulator of placental and fetal growth. *Nature*, **417**, 945–948.
23. Fowden,A.L., Ward,J.W., Wooding,F.P., Forhead,A.J. and Constancia,M. (2006) Programming placental nutrient transport capacity. *J. Physiol.*, **572**, 5–15.
24. Gabory,A., Ripoche,M.A., Yoshimizu,T. and Dandolo,L. (2006) The H19 gene: regulation and function of a non-coding RNA. *Cytogenet. Genome Res.*, **113**, 188–193.
25. Su,A.I., Wiltshire,T., Batalov,S., Lapp,H., Ching,K.A., Block,D., Zhang,J., Soden,R., Hayakawa,M., Kreiman,G. *et al.* (2004) A gene atlas of the mouse and human protein-encoding transcriptomes. *Proc. Natl Acad. Sci. USA*, **101**, 6062–6067.
26. Kim,S.J., Park,S.E., Lee,C., Lee,S.Y., Kim,I.H., An,H.J. and Oh,Y.K. (2003) Altered imprinting, promoter usage, and expression of insulin-like growth factor-II gene in gestational trophoblastic diseases. *Gynecol. Oncol.*, **88**, 411–418.
27. Jinno,Y., Ikeda,Y., Yun,K., Maw,M., Masuzaki,H., Fukuda,H., Inuzuka,K., Fujishita,A., Ohtani,Y., Okimoto,T. *et al.* (1995) Establishment of functional imprinting of the H19 gene in human developing placentae. *Nature Genet.*, **10**, 318–324.
28. Tost,J., Dunker,J. and Gut,I.G. (2003) Analysis and quantification of multiple methylation variable positions in CpG islands by Pyrosequencing. *Biotechniques*, **35**, 152–156.
29. Dupont,J.M., Tost,J., Jammes,H. and Gut,I.G. (2004) De novo quantitative bisulfite sequencing using the pyrosequencing technology. *Anal. Biochem.*, **333**, 119–127.
30. Tost,J., El Abdalaoui,H. and Gut,I.G. (2006) Serial pyrosequencing for quantitative DNA methylation analysis. *Biotechniques*, **40**, 721–726.
31. Tost,J., Schatz,P., Schuster,M., Berlin,K. and Gut,I.G. (2003) Analysis and accurate quantification of CpG methylation by MALDI mass spectrometry. *Nucleic Acids Res.*, **31**, e50.
32. Sparago,A., Cerrato,F., Vernucci,M., Ferrero,G.B., Silengo,M.C. and Riccio,A. (2004) Microdeletions in the human H19 DMR result in loss of IGF2 imprinting and Beckwith-Wiedemann syndrome. *Nature Genet.*, **36**, 958–960.

33. Prawitt,D., Enklaar,T., Gartner-Rupprecht,B., Spangenberg,C., Oswald,M., Lausch,E., Schmidtke,P., Reutzel,D., Fees,S., Lucito,R. *et al.* (2005) Microdeletion of target sites for insulator protein CTCF in a chromosome 11p15 imprinting center in Beckwith-Wiedemann syndrome and Wilms' tumor. *Proc. Natl Acad. Sci. USA*, **102**, 4085–4090.

34. Feil,R., Walter,J., Allen,N.D. and Reik,W. (1994) Developmental control of allelic methylation in the imprinted mouse Igf2 and H19 genes. *Development*, **120**, 2933–2943.

35. De Castro Valente Esteves,L.I., De Karla Cervigne,N., Do Carmo Javaroni,A., Magrin,J., Kowalski,L.P., Rainho,C.A. and Rogatto,S.R. (2006) H19-DMR allele-specific methylation analysis reveals epigenetic heterogeneity of CTCF binding site 6 but not of site 5 in head-and-neck carcinomas: a pilot case-control analysis. *Int. J. Mol. Med.*, **17**, 397–404.

36. Richards,E.J. (2006) Inherited epigenetic variation--revisiting soft inheritance. *Nature Rev. Genet.*, **7**, 395–401.

37. Morgan,H.D., Sutherland,H.G., Martin,D.I. and Whitelaw,E. (1999) Epigenetic inheritance at the agouti locus in the mouse. *Nature Genet.*, **23**, 314–318.

38. Rakyan,V.K., Chong,S., Champ,M.E., Cuthbert,P.C., Morgan,H.D., Luu,K.V. and Whitelaw,E. (2003) Transgenerational inheritance of epigenetic states at the murine Axin(Fu) allele occurs after maternal and paternal transmission. *Proc. Natl Acad. Sci. USA*, **100**, 2538–2543.

39. Hitchins,M., Williams,R., Cheong,K., Halani,N., Lin,V.A., Packham,D., Ku,S., Buckle,A., Hawkins,N., Burn,J. *et al.* (2005) MLH1 germline epimutations as a factor in hereditary nonpolyposis colorectal cancer. *Gastroenterology*, **129**, 1392–1399.

40. Suter,C.M., Martin,D.I. and Ward,R.L. (2004) Germline epimutation of MLH1 in individuals with multiple cancers. *Nature Genet.*, **36**, 497–501.

41. Lewis,A., Mitsuya,K., Umlauf,D., Smith,P., Dean,W., Walter,J., Higgins,M., Feil,R. and Reik,W. (2004) Imprinting on distal chromosome 7 in the placenta involves repressive histone methylation independent of DNA methylation. *Nature Genet.*, **36**, 1291–1295.

42. Umlauf,D., Goto,Y., Cao,R., Cerqueira,F., Wagschal,A., Zhang,Y. and Feil,R. (2004) Imprinting along the Kcnq1 domain on mouse chromosome 7 involves repressive histone methylation and recruitment of Polycomb group complexes. *Nature Genet.*, **36**, 1296–1300.